

Quantum oscillations of the superconductor LaRu_2P_2 : Comparable mass enhancement $\lambda \approx 1$ in Ru and Fe phosphides

Philip J. W. Moll,¹ Jakob Kanter,¹ Ross D. McDonald,² Fedor Balakirev,² Peter Blaha,³ Karlheinz Schwarz,³ Zbigniew Bukowski,¹ Nikolai D. Zhigadlo,¹ Sergiy Katrych,¹ Kurt Mattenberger,¹ Janusz Karpinski,¹ and Bertram Batlogg¹

¹Laboratory for Solid State Physics, ETH Zurich, Switzerland

²National High Magnetic Field Laboratory, Los Alamos National Laboratory, MS-E536, Los Alamos, New Mexico 87545, USA

³Institute of Materials Chemistry, Vienna University of Technology, A-1040 Vienna, Austria

(Received 1 November 2011; published 15 December 2011)

We have studied the angular-dependent de Haas-van Alphen oscillations of LaRu_2P_2 using magnetic torque in pulsed magnetic fields up to 60 T. The observed oscillation frequencies are in excellent agreement with the geometry of the calculated Fermi surface. The temperature dependence of the oscillation amplitudes reveals effective masses $m^*(\alpha) = 0.71$ and $m^*(\beta) = 0.99 m_e$, which are enhanced over the calculated band mass by λ^{vc} of 0.8. We find a similar enhancement of $\lambda^\gamma \approx 1$ in comparing the measured electronic specific heat ($\gamma = 11.5 \text{ mJ/mol K}^2$) with the total density of states from band-structure calculations. Remarkably, very similar mass enhancements have been reported in other pnictides, LaFe_2P_2 , LaFePO ($T_c \approx 4 \text{ K}$), and LaRuPO , independent of whether they are superconducting or not. This is contrary to the common perceptions that the normal-state quasiparticle renormalizations reflect the strength of the superconducting pairing mechanism and leads to new questions about pairing in isostructural and isoelectronic Ru- and Fe-pnictide superconductors.

DOI: [10.1103/PhysRevB.84.224507](https://doi.org/10.1103/PhysRevB.84.224507)

PACS number(s): 71.18.+y, 74.70.Xa

I. INTRODUCTION

Electronic correlations and the associated electron mass enhancements are central aspects in the discussion of superconductivity in transition-metal compounds.¹ Correlations are of particular importance in unconventional superconductors such as the cuprates and pnictides, which are not dominated by electron-phonon coupling.² As superconductivity in the pnictides can be tuned by changing various parameters such as carrier doping^{3,4} and chemical^{5,6} and external pressure,^{7,8} valuable insights on the pairing mechanism may be gained by direct comparison of closely related systems. A particularly intriguing situation presents itself when two seemingly similar pairs of isostructural and isoelectronic compounds and their superconductivity are compared: LaRu_2P_2 - LaFe_2P_2 and LaRuPO - LaFePO : While, in the former, LaRu_2P_2 is superconducting ($T_c = 4 \text{ K}$) and LaFe_2P_2 is not, in the latter the roles of Fe(3d) and Ru(4d) are interchanged and LaFePO is superconducting ($T_c = 4 \text{ K}$) while LaRuPO is not. To approach this puzzle, we study in detail the electronic structure near E_F and the enhancement of the quasiparticle mass over the calculated bare band mass.

II. EXPERIMENTAL

Experimentally, we have measured quantum oscillations in LaRu_2P_2 single crystals by means of torque magnetometry in high magnetic fields up to 60 T. Quantum oscillations are precise bulk tools to identify the Fermi surface (FS) geometry and to measure band-specific effective masses on the extremal orbits.⁹ Furthermore, we have measured the heat capacity to determine the electronic density of states (DOS) at E_F . Theoretically, we have calculated the electronic band structure of LaRu_2P_2 and LaFe_2P_2 using the density-functional-theory (DFT) code WIEN2k^{10,11} to identify similarities and differences. Importantly, the comparison of quantum oscillations, specific-heat data, and band calculations allows us to estimate

the individual band contributions to the many-body mass enhancement.

Single crystals of LaRu_2P_2 were grown by the Sn flux method using LaP_2 and Ru powders as starting materials, similar to other “122” pnictides.¹² The components (1:2:2:40 La:Ru:P:Sn ratio) were loaded into an alumina crucible and sealed in an evacuated silica tube. The ampoule was kept at 1100°C for 12 h, slowly cooled to 750°C at $1.5\text{--}2^\circ\text{C/h}$, followed by fast cooling to room temperature. The Sn matrix was dissolved in hydrochloric acid. Powder x-ray-diffraction analysis performed on crushed crystals confirmed the ThCr_2Si_2 -type structure with the lattice parameters $a = 4.025 \text{ \AA}$ and $c = 10.662 \text{ \AA}$. We have studied three individual crystals from the same growth batch. The large crystals were cut into suitable pieces of about $200 \times 100 \times 40 \mu\text{m}$ in size. Crystals 1 and 2 were studied as grown, while crystal 3 was sealed in a quartz ampoule and annealed in vacuum at 800°C for 10 days to further improve the crystal quality. All three crystals gave quantum oscillations of the same frequency and of comparable amplitude. The in-plane residual resistivity ratio $\rho(300 \text{ K})/\rho(5 \text{ K})$ was typically about 20 (Fig. 1). Polycrystalline samples of LaFe_2P_2 were prepared under high pressure (30 kbar) at 1400°C , and phase purity was checked by x-ray. The high-field measurements up to 60 T with a pulse duration of 200 ms were performed at the National High Magnetic Field Laboratory. The sample was glued to a commercial piezoresistive microcantilever (SEIKO PRC-120, lower left inset, Fig. 1). These devices detect sensitively oscillations in the magnetic torque $\tau \propto M \times H$.¹³ The cantilever resistance was measured in a balanced Wheatstone configuration at 297.5 kHz.

Figure 2(a) shows the raw torque signal with a tilt angle of $\theta = 20^\circ$ between the field and the crystallographic c axis (perpendicular to the Ru-P layers) at temperatures between 5 and 18 K. The weakly paramagnetic background is subtracted using a smooth polynomial of third order to obtain the

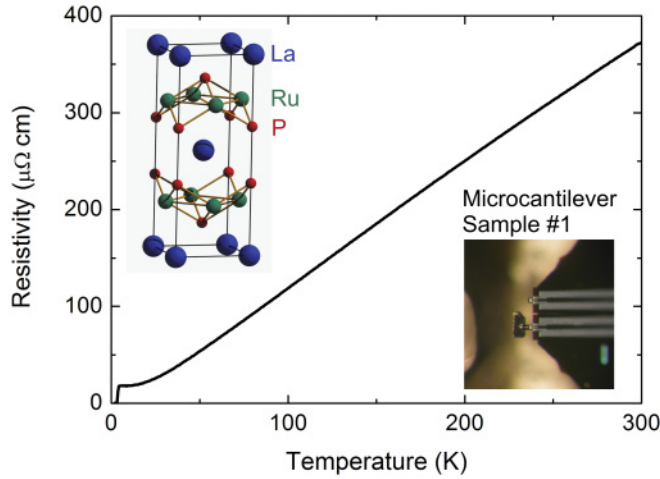


FIG. 1. (Color online) In-plane resistivity of a typical LaRu_2P_2 single crystal as a function of temperature. The four-point resistivity begins to saturate below 20 K, giving a residual resistivity ratio of 21. Left inset: LaRu_2P_2 unit cell (ThCr_2Si_2 type). Right inset: sample 1 mounted on a SEIKO cantilever.

oscillatory part of the torque and to suppress $1/f$ noise in the Fourier spectrum [Fig. 2(b)]. At this angle, we find two main frequency components, α (349 T) and β (1921 T). The reduction of the oscillation amplitudes A with increasing temperature due to the broadening of the Fermi-Dirac distribution is well described by the Lifshitz-Kosevich formalism, $A/A_0 = X/\sinh(X)$ with $X = 2\pi^2 k_B T/\hbar\omega_c$ [Fig. 2(c)]. From this fit, we extract effective masses m^* for the two orbits as $m_\alpha^* = 0.71 m_e$ and $m_\beta^* = 0.99 m_e$. While these appear to be light masses, these values have to be compared later with calculated bare band masses.

Now we turn to the FS geometry. The frequencies F are directly connected to the k -space area S_k encompassed by an extremal cyclotron orbit on the FS perpendicular to the applied field via the Onsager relation $F = 2\pi e S_k/\hbar$. Thus, studying the angular dependence of the frequencies allows to determine the bulk FS tomographically. The rotation axis was aligned with the crystal facet perpendicular to the a - or equivalent b axis, to select a magnetic-field rotation from the c axis ($\theta = 0^\circ$) to the a axis ($\theta = 90^\circ$). The frequencies of all three studied samples agree very well and are given in Fig. 2(d). At small angles, the spectrum is given by the low-lying α and the higher β and β' frequencies. At higher angles, between 40 and 50° , the spectrum changes and only one frequency γ is present.

III. BAND STRUCTURE CALCULATION

To interpret this data, we have performed electronic band-structure calculations using WIEN2k and the generalized gradient approximation by Perdew *et al.* (PBE-GGA).¹⁴ The LaRu_2P_2 structure was calculated from experimental x-ray data¹⁵ without lattice relaxation, as no notable forces on the atoms resulted from the use of these coordinates. The calculated Fermi surface of LaRu_2P_2 is given in Fig. 3(a). Three bands cross E_F and produce three FS sheets: (1) a donut with a small hole centered around the M point (outside: turquoise; inside: red), (2) a warped electron cylinder around

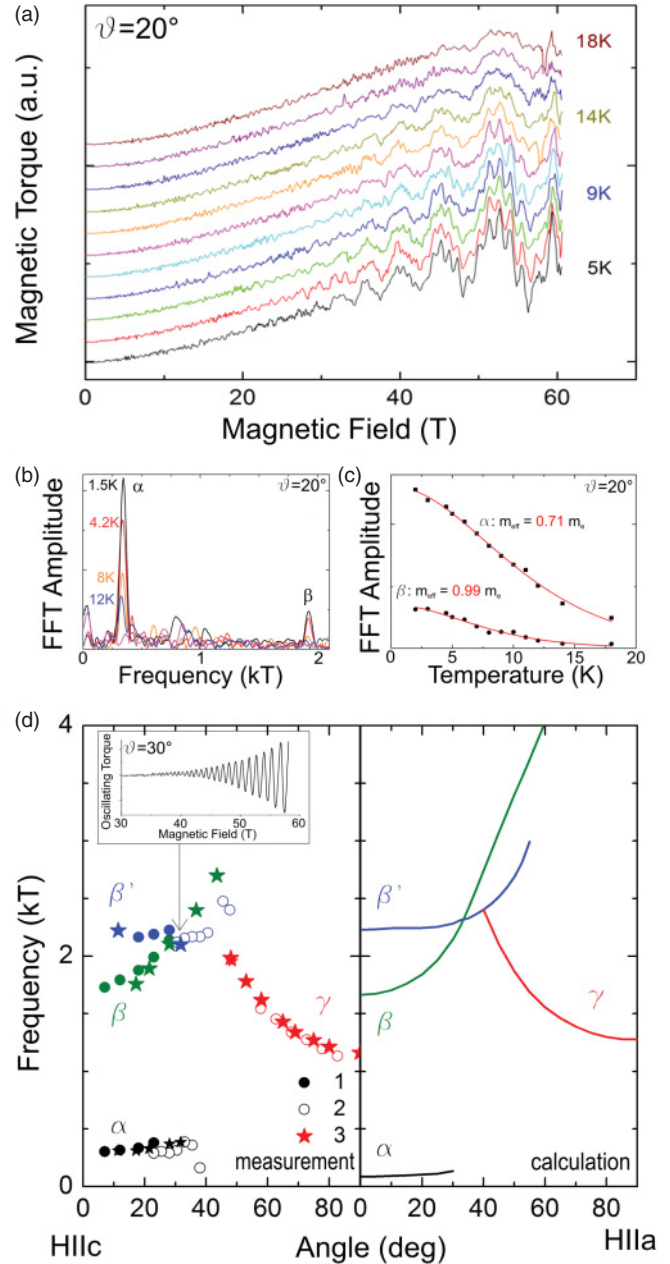


FIG. 2. (Color) (a) Raw torque signal measured at various temperatures between 18 and 5 K at an angle $\theta = 20^\circ$ between the field and c axis (curves are offset for clarity). The quantum oscillations are clearly visible at the high temperature of 18 K, indicating the light effective masses on these orbits. (b) Frequency spectrum of this data. (c) Temperature dependence of the oscillatory torque amplitudes ($\theta = 20^\circ$), originating from the α (donut hole) and β (cylinder) orbits. The line shows a fit to the Lifshitz-Kosevich formula. (d) Measured and calculated angular dependence of the amplitudes. The good agreement allows for the identification of orbits on the FS.

the zone corners (outside: green; inside: purple), and (3) a strongly folded three-dimensional open FS (for clarity, moved to the side: blue and yellow).

From these FS geometries we calculate the extremal cross sections for the various angles and express them as quantum oscillation frequencies, shown in Fig. 2(d). The

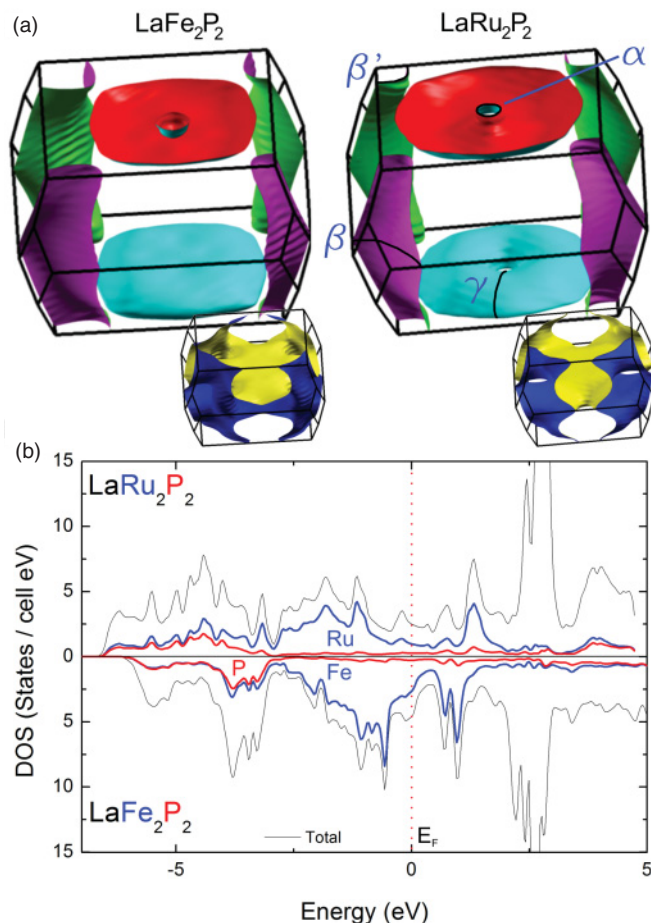


FIG. 3. (Color) (a) Fermi surfaces of LaFe₂P₂ and LaRu₂P₂ calculated by DFT. The orbits observed in the dHvA experiments in LaRu₂P₂ have been labeled. (b) Density-of-states comparison between the Fe and Ru compounds. The more localized Fe 3d states cause in LaFe₂P₂ a smaller bandwidth and a larger DOS at the Fermi level.

good agreement between calculated and measured frequencies allows us to identify them with orbits on the FS. The β and β' orbits correspond to the neck and belly of the cylinder around X . These two frequencies get closer at higher angles and finally cross at a Yamaji angle^{9,16} of $\theta = 30^\circ$ [marked in Fig. 2(d)]. This is very close to the calculated value of 33° , and the excellent agreement is a strong indication that the calculation accurately reproduces the warping of the

cylinder. The cylinder corresponds to the hybridized Ru-4d, P-2p in-plane bonds and is a common feature in tetragonal 122 pnictide superconductors (e.g., Refs. 17–19). The γ branch between 50 and 90° agrees within a few percent with the cross-sectional orbit of the donut FS. The α orbit corresponds to the small donut hole, which is about 3.5 times larger in area than calculated. The hole diameter is very sensitive to shifts of the Fermi energy and can be reconciled with the data by a small energy shift of about 40 meV.

The measured mass m_β of $0.99 m_e$ is light compared to the masses of the electron cylinders centered at X in other isostructural 122 phosphorus compounds: $m^*/m_e = 1.5$ (BaNi₂P₂¹⁸), 2.05 (CaFe₂P₂ in collapsed-tetragonal phase¹⁹), and 1.6–2.1 (SrFe₂P₂¹⁷). Interestingly, BaFe₂As₂, the parent compound of the (Ba, K) Fe₂As₂ high-temperature superconductor, shows similar light masses around $0.9 m_e$ ²⁰ in the orthorhombic low-temperature phase.²¹

IV. DISCUSSION

To better understand the inherent difference between the Fe and Ru analogs, we have contrasted in Fig. 3 the calculated electronic structure of LaFe₂P₂ and LaRu₂P₂. The two FSs are indeed very similar, where the former has a slightly thicker cylinder and the donut hole becomes a topologically disconnected sphere enclosed in a solid pillow. Differences in the electronic structure, however, become evident when the overall band structure is considered. In Fig. 3(b) we contrast the DOS of the two materials. The replacement of Fe-3d by less localized Ru-4d orbitals increases the bandwidth and thus lowers the overall DOS. At the Fermi level, we calculate 4.60 states/eV in LaFe₂P₂ and 2.46 states/eV in LaRu₂P₂. These values correspond to a linear electronic heat coefficient γ^{calc} of 5.8 mJ/mol K² in LaRu₂P₂ and 10.8 mJ/mol K² in LaFe₂P₂. In LaRu₂P₂ we have measured a γ^{exp} of 11.5 mJ/mol K², giving a mass enhancement factor λ^γ defined as $\gamma^{\text{exp}}/\gamma^{\text{calc}} = (1 + \lambda^\gamma)$ of 0.98. Similarly in LaFe₂P₂ we find a γ^{exp} of 19.3 mJ/mol K² and λ^γ of 0.8.

This should be compared to the effective mass enhancement of orbits on individual FS sheets $m_{\text{exp}}/m_b = (1 + \lambda^{\text{cyc}})$. We have extracted the band cyclotron mass m_b for each orbit S_k and field angle from our calculated band structure using the relation $m_b = \hbar/2\pi e dS_k/dE|_{E_F}$. At $\theta = 20^\circ$, we find $m_b^\alpha = 0.40 m_e$ and $m_b^\beta = 0.55 m_e$ leading to a mass enhancement λ^{cyc} of 0.78 for α and 0.8 for β . If the small difference between

TABLE I. Mass enhancement from cyclotron mass and specific heat in Fe and Ru pnictides.

Material	Measured cyclotron mass (m/m _e)	Renormalization λ^{cyc} from cyc. mass	Measured specific heat γ (mJ/mol K ²)	Calculated γ (mJ/mol K ²)	Renormalization λ^γ from γ
LaRu ₂ P ₂	0.71, 0.99	0.8	11.5	5.8	1
LaFe ₂ P ₂	2.0, 2.7 ²²		19.3	10.8	0.8
LaRuPO	0.55–0.86 ²²		3.9 ²³	2	0.95
LaFePO	1.8–2.1 ²⁴	1 ²⁴	12.5 ²⁵	6	1.08
BaFe ₂ As ₂ ²⁰	0.6–1.2	0.7–1	6.1	2.83	1.1
SrFe ₂ As ₂ ²⁶	1.5, 2.0	0.85	3.3	1.9	0.74
CaFe ₂ P ₂	2.05–4.0 ¹⁹	0.45–0.51 ¹⁹	6.5 ²⁷		
BaNi ₂ P ₂ ¹⁸	0.53–1.50	0.3–2.1		8.78	

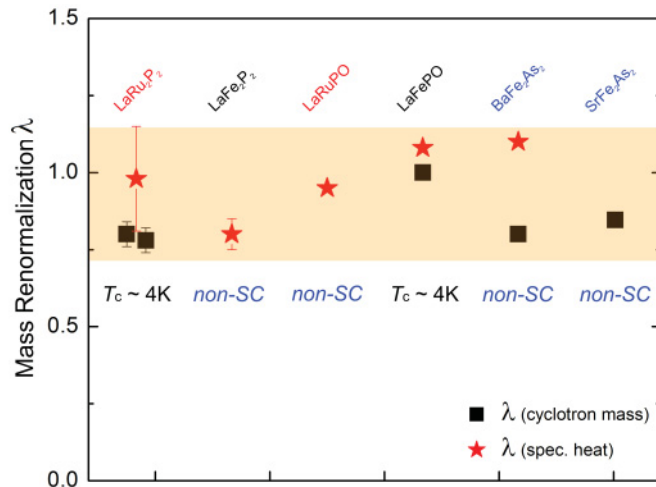


FIG. 4. (Color online) Mass renormalization λ of LaRu₂P₂ and other related compounds, determined by quantum oscillations and specific-heat measurements. For all these materials λ is similar, around 1.

λ^{cyc} and $\lambda^{\text{spec. heat}}$ is taken literally, it suggests that the unobserved three-dimensional sheet is more renormalized compared to the donut and cylinder sheets.

Overall, this yields a highly consistent picture of similar mass enhancements with $\lambda \approx 1$ in the iron-pnictide compounds upon Ru substitution, even as LaRu₂P₂ and LaFePO are superconductors and LaFe₂P₂ and LaRuPO are not (sketched in Fig. 4 and Table I). The substitution of Fe for Ru was recently studied by angle-resolved photoemission spectroscopy measurements,²⁸ and it was suggested to reduce the electronic correlations in the 122 pnictides. It is impossible in de Haas-van Alphen (dHvA) experiments to separate the electron-electron interaction enhancement from the electron-phonon contribution. However, because the

total mass renormalization is similar in the Ru and the Fe compounds, it would be a remarkable coincidence that the reduction of electronic correlations due to the broader Ru bands would be compensated by an equivalent increase in electron-phonon interactions. It will be of interest to compare these mass renormalizations at E_F with the optically probed mass enhancement at higher energies.¹

V. CONCLUSION

In conclusion, our dHvA studies and specific-heat measurements reveal that local-density approximation calculations reproduce the band structure of LaRu₂P₂ in great detail and give highly similar Fermi surfaces for LaRu₂P₂ and LaFe₂P₂. Thus, differences in FS nesting are unlikely to be the explanation for the appearance of superconductivity in LaRu₂P₂. A similar, sizable quasiparticle mass renormalization of $\lambda \approx 1$ is found in both discussed pairs LaRu₂P₂ ($T_c = 4$ K)-LaFe₂P₂ and LaRuPO-LaFePO ($T_c = 4$ K), as well as other pnictides. This similar mass enhancement observed in both superconducting and nonsuperconducting pnictides is contrary to the common perceptions that the normal state quasiparticle renormalizations reflect the strength of the superconducting pairing mechanism.

ACKNOWLEDGMENTS

This work was supported by the Swiss National Science Foundation and the National Center of Competence in Research MaNEP (Materials with Novel Electronic Properties). Work at the National High Magnetic Field Laboratory is carried out under the auspices of the National Science Foundation, Department of Energy, and State of Florida. P. B. was supported by the Austrian Science Fund SFB-F41 (ViCoM).

¹M. M. Quasibash *et al.*, *Nature Physics* **5**, 647 (2009).

²L. Boeri, M. Calandra, I. I. Mazin, O. V. Dolgov, and F. Mauri, *Phys. Rev. B* **82**, 020506 (2010).

³Y. Kamihara *et al.*, *J. Am. Chem. Soc.* **128**, 10012 (2006).

⁴J. Yang *et al.*, *Supercond. Sci. Technol.* **22**, 025004 (2009).

⁵C. Wang *et al.*, *Europhys. Lett.* **86**, 47002 (2009).

⁶M. Tropeano, C. Fanciulli, F. Canepa, M. R. Cimberle, C. Ferdeghini, G. Lamura, A. Martinelli, M. Putti, M. Vignolo, and A. Palenzona, *Phys. Rev. B* **79**, 174523 (2009).

⁷H. Okada *et al.*, *J. Phys. Soc. Jpn.* **77**, 113712 (2008).

⁸C. W. Chu and B. Lorenz, *Physica C: Superconductivity* **469**, 385 (2009).

⁹D. Shoenberg, *Magnetic Oscillations in Metals*, 1st ed. (Cambridge University Press, Cambridge, 2009).

¹⁰P. Blaha *et al.*, *WIEN2k: An Augmented Plane Wave and Local Orbitals Program for Calculating Crystal Properties* (Vienna University of Technology, Wien, Austria, 2001).

¹¹K. Schwarz *et al.*, *Mol. Phys.* **108**, 3147 (2010).

¹²Z. Bukowski, S. Weyeneth, R. Puzniak, P. Moll, S. Katrych, N. D. Zhigadlo, J. Karpinski, H. Keller, and B. Batlogg, *Phys. Rev. B* **79**, 104521 (2009).

¹³E. Ohmichi *et al.*, *Rev. Sci. Instrum.* **73**, 3022 (2002).

¹⁴J. P. Perdew, K. Burke, and M. Ernzerhof, *Phys. Rev. Lett.* **77**, 3865 (1996).

¹⁵W. Jeitschko *et al.*, *J. Solid State Chem.* **69**, 93 (1987).

¹⁶K. Yamaji, *J. Phys. Soc. Jpn.* **58**, 1520 (1989).

¹⁷J. G. Analytis, C. M. J. Andrew, A. I. Coldea, A. McCollam, J. H. Chu, R. D. McDonald, I. R. Fisher, and A. Carrington, *Phys. Rev. Lett.* **103**, 76401 (2009).

¹⁸T. Terashima *et al.*, *J. Phys. Soc. Jpn.* **78**, 033706 (2009).

¹⁹A. I. Coldea, C. M. J. Andrew, J. G. Analytis, R. D. McDonald, A. F. Bangura, J. H. Chu, I. R. Fisher, and A. Carrington, *Phys. Rev. Lett.* **103**, 026404 (2009).

²⁰J. G. Analytis, R. D. McDonald, J. H. Chu, S. C. Riggs, A. F. Bangura, C. Kucharczyk, M. Johannes, and I. R. Fisher, *Phys. Rev. B* **80**, 064507 (2009).

- ²¹Q. Huang, Y. Qiu, W. Bao, M. A. Green, J. W. Lynn, Y. C. Gasparovic, T. Wu, G. Wu, and X. H. Chen, *Phys. Rev. Lett.* **101**, 257003 (2008).
- ²²H. Muranaka *et al.*, *J. Phys. Soc. Jpn.* **78**, 053705 (2009).
- ²³C. Krellner, N. S. Kini, E. M. Bruning, K. Koch, H. Rosner, M. Nicklas, M. Baenitz, and C. Geibel, *Phys. Rev. B* **76**, 104418 (2007).
- ²⁴A. I. Coldea, J. D. Fletcher, A. Carrington, J. G. Analytis, A. F. Bangura, J. H. Chu, A. S. Erickson, I. R. Fisher, N. E. Hussey, and R. D. McDonald, *Phys. Rev. Lett.* **101**, 216402 (2008).
- ²⁵T. M. McQueen, M. Regulacio, A. J. Williams, Q. Huang, J. W. Lynn, Y. S. Hor, D. V. West, M. A. Green, and R. J. Cava, *Phys. Rev. B* **78**, 024521 (2008).
- ²⁶S. E. Sebastian *et al.*, *J. Phys. Condens. Matter* **20**, 422203 (2008).
- ²⁷G. F. Chen, Z. Li, J. Dong, G. Li, W. Z. Hu, X. D. Zhang, X. H. Song, P. Zheng, N. L. Wang, and J. L. Luo, *Phys. Rev. B* **78**, 224512 (2008).
- ²⁸V. Brouet *et al.*, *Phys. Rev. Lett.* **105**, 087001 (2010).